Journal of Virological Methods 218 (2015) 71–76

Contents lists available at ScienceDirect

Journal of Virological Methods

journal homepage: www.elsevier.com/locate/jviromet

Characterization of vesicular stomatitis virus populations by tunable resistive pulse sensing

Fulya Akpinar*, John Yin

Department of Chemical and Biological Engineering, Systems Biology Theme, Wisconsin Institute for Discovery, University of Wisconsin-Madison, Madison, WI 53706, USA

Article history:
Received 23 August 2014
Received in revised form
30 November 2014
Accepted 9 February 2015
Available online 16 February 2015

Keywords:
Coulter counter
Particle quantification
Virus populations characterization
Tunable resistive pulse sensing
Vesicular stomatitis virus

A B S T R A C T

Although transmission electron microscopy (TEM) has historically been the method of choice to estimate concentrations of virus and virus-like particles, these measures can often be time-consuming and labor-intensive to perform. Tunable resistive pulse sensing (TRPS) is an emerging method that applies principles of Coulter counting to nanoscale particles and may provide a simpler and higher-throughput alternative to TEM for the quantitation of virus populations. To assess the performance of TRPS compared to TEM, the samples of polymer spheres at a diameter of 100 nm and vesicular stomatitis virus (VSV) were characterized using both techniques. TRPS was able to quantify concentrations down to 10^7 particles/ml, providing nearly 50-fold larger measurement range, and more reproducible counts than TEM. Total-to-infectious particle ratio of VSV populations as measured by TRPS and plaque assay suggested that each VSV particle is infectious. In addition to particle counts, TRPS successfully measured particle size distributions based on hundreds of particles. Such high throughput sustained by TRPS can assist quantitative characterization of virus populations.

1. Introduction

The total-to-infectious particle ratio is a useful measure of how efficiently virus particles infect cells. The ratio has been estimated traditionally by dividing the total particle concentration measured via transmission electron microscopy (TEM) by the infectious unit concentration, as determined by plaque assay (Galasso and Sharp, 1962; Carpenter et al., 2009). TEM allows for direct visualization and quantitation of virus particles, but it requires significant time and effort for sample preparation, imaging and image analysis (Watson et al., 1963).

As an alternative to electron microscopy, particle quantitation devices based on Coulter principles, known as Coulter counters have been developed, which provide a simple, high-throughput and inexpensive platform for single particle analysis (DeBlois, 1970; Henriquez et al., 2004; Kozak et al., 2011). Typically, a Coulter counter is composed of two fluid reservoirs filled with conductive media and separated by a membrane which has a pore. This pore allows only the particles that are smaller than the pore diameter to pass through. When an electrical field is applied across the pore, the resistance to the resulting ionic current is indirectly proportional to the cross sectional area of the pore. When a non-conducting particle passes through the pore, the increase in resistance is proportional to the particle volume relative to (pore size)^4. This change in resistance is detected as a pulse in ionic current. The pulse frequency is proportional to particle flow rate and thus to particle concentration.

Recently, the usage of tunable pores in Coulter counters, as in tunable resistive pulse sensing (TRPS) technology, has allowed sensitive measurements of a broad size range of particles (Kozak et al., 2011; Vogel et al., 2011). In comparative studies of particle characterization techniques (Bell et al., 2012; Anderson et al., 2013; Heider and Metzner, 2014), TRPS has shown advantages over other techniques due to its ability for simultaneous particle sizing and counting, and its higher accuracy in polydisperse particle sizing as compared to commonly used techniques such as nanoparticle tracking analysis and dynamic light scattering (Anderson et al., 2013; Terejanszky et al., 2014). The success of TRPS in particle quantitation has sparked its applications in the characterization of biological nanoparticles including virus populations (Vogel et al., 2011; Gazzola et al., 2012; Van Bracht et al., 2012; Arjmandi et al., 2014). While the applications of TRPS in the characterization of virus infections continue to expand, its accuracy in the quantitation of virus populations has not been fully tested.

* Corresponding author at: 330N. Orchard Street, Madison, WI 53715, USA. Tel.: +1 608 316 4323.
E-mail addresses: akpinar@uwalumni.com (F. Akpinar), john.yin@wisc.edu (J. Yin).

http://dx.doi.org/10.1016/j.jviromet.2015.02.006
0166-0934/

To address the need for the validation of the accuracy of TRPS in quantitative analysis of virus populations, in this study, the performance of TRPS in characterizing spherical polymer nanoparticles and vesicular stomatitis virus (VSV) populations was compared with that of TEM. As a bullet shaped virus, VSV allowed testing the accuracy of both techniques in the characterization of non-spherical particles with high aspect ratio (length-to-width ratio). The results demonstrated the ability of TRPS to quantify the concentration and size distribution of both spherical nanoparticle and non-spherical VSV populations.

2. Material and methods

2.1. Cell and virus culture

Baby hamster kidney (BHK-21) cells were cultured at 37 °C and 5% CO_2 in Eagle's minimum essential medium (MEM; Mediatech-CellGro, Herndon, VA, USA) with 1% Glutamax I (Life Technologies, Carlsbad, CA, USA) and 10% fetal bovine serum (FBS, Atlanta Biologicals, Norcross, GA, USA). The culture medium was switched to medium with the 2% FBS for all virus infections. A well-defined virus strain based on the Indiana serotype of Vesicular stomatitis virus (VSV), VSV-N1 (Wertz, 1998), was used for infections. VSV is from order *Mononegavirales*, family *Rhabdoviridae*, genus *Vesiculovirus.* To prepare virus stock, BHK-21 cells were infected with plaque purified virus diluted to 0.001 plaque forming units (PFU) per cell in a T-75 flask (Falcon, BD Biosciences, San Jose, CA, USA), incubated for 24 h at 37 °C, filtered with a 0.22 mm filter (Millipore, Bedford, MA, USA), and stored at −80 °C.

2.2. Plaque assay

Virus was quantified by plaque assay. The day prior to infection, cells were removed from T-75 flasks by treating with Trypsin EDTA (CellGro, Herdon, VA, USA). The cells were diluted in 10% FBS media to 10^5 cells/ml. Two ml of the cell solution were pipetted into each well of 6-well tissue culture treated polystyrene plates (Corning, New York, USA). The virus samples were thawed at room temperature and serial 10-fold dilutions were prepared in MEM. The media above the cell monolayer was removed, rinsed with Dulbecco's Phosphate-Buffered Saline (DPBS; Gibco, Life Technologies, New York, USA) and the cells were infected with 200 μl of the virus suspension and incubated for 1 h. The inoculum was removed and the cells were overlaid with 2 ml of 0.6% (w/v) agar (Difco, Becton Dickson, Sparks, MD, USA) diluted in 2% FBS infection medium. After 20 h of incubation, the agar overlay was removed and cells were fixed in 4% (w/v) paraformaldahyde (PFA, MP Biomedicals, Solon, OH, USA) and 5% (w/v) sucrose solution. The fixative remained on the cells for 20 min and then the cells were rinsed twice with DPBS and stained with 2.5% (v/v) crystal violet (CV; PML Microbiological, Wilsonville, USA) diluted in 20% ethanol to aid in visualizing plaques. After the CV dried plaques were counted, virus titers were calculated as PFU/ml.

2.3. Microsphere standards

The particle counts by both TEM and TRPS were calibrated with the dilutions of carboxylated polystyrene microspheres with a nominal diameter of 100 nm (Polybead series, Polysciences, Warrington, PA, USA) and a concentration of 10^{10} particles/ml. Only for the determination of the size distributions by TEM, unmodified polystyrene beads (NIST traceable size standards; Thermo Fisher Scientific, Fremont, CA, USA) with nominal diameters of 102 nm and 10^9 particles/ml was used. Both calibration samples were tested by independent TEM measurements (Smith and Melnick, 1962). To test the size measurements by TRPS, carboxylated polystyrene microspheres with a nominal diameter of 70 nm and 110 nm (BANGS, Fishers, IN, USA) were measured. The counts were calibrated with aforementioned calibration beads.

2.4. Particle quantitation by transmission electron microscopy

The virus samples were mixed with microsphere calibration standards in 1:1 ratio. The prepared mixture was diluted 1:1 with methylamine tungstate (Nanoprobes, Yaphank, NY, USA) and a drop was loaded on a pioloform coated grid. The samples were then imaged using a TEM (CM120, Philips, Netherlands). 15 TEM images were acquired for each sample, and VSV particles and microspheres were counted and averaged. The VSV particle concentration was estimated relative to the concentration of calibration microspheres. The polystyrene microsphere samples were imaged in a similar manner. Instead of calibrating the counts with a reference particle sample, Smith and Melnick method was used to quantify the particle concentrations (Smith and Melnick, 1962). The dimensions of virus particles and microspheres were measured using the software iTEM (Olympus, Münster, Germany).

2.5. TRPS measurements

Virus particles and carboxylated polystyrene microspheres were quantified using a commercial TRPS instrument (qViro, IZON Science, Christchurch, New Zealand). MEM was used as electrolyte. Both microsphere and virus samples were diluted to appropriate levels in MEM with a great care in pipetting and vortexing. A TPU membrane, on which a tunable nanopore was punctured and mounted on TRPS to 100 nm pore size (NP100, IZON Science Christchurch, New Zealand) (Sowerby et al., 2007), was placed on the lower well and stretched to allow particle passage. 75 μl MEM was pipetted into the lower well and the upper well was set on the top of the membrane. 40 μl test sample was added to the upper fluid well. A continuous flow of particles was maintained by adjusting the pore stretch and the voltage. A minimum of 5 particles/min was targeted. A pressure of 10 cm-H_2O was established across the nanopore to minimize the effect of particle surface charge on concentration measurements. To avoid nanopore clogging and serial contamination between sample runs, a blank MEM buffer was run through the pore between the measurements of each sample. Current pulse signals were acquired over 2 min using the IZON Control Suite 2.2. Later the same software was used to process the recorded data. The particle concentration and size distribution was estimated by comparing the particle flow rate and signal magnitudes of the test sample with that of the calibration sample described before. The average size and concentration of calibration sample was entered as the basis of size and concentration calculations.

3. Results

3.1. Quantitation of the concentration and size distributions of microspheres by TRPS

To test the ability of TRPS to measure the size and concentration of nanoparticles and to determine its detection range, the carboxylated polystyrene microspheres were diluted to different concentrations and analyzed by TRPS. Fig. 1 shows a subset of the current signal (yellow line) recorded for three different dilutions of microspheres. Each downward pulse in current signal indicates a single particle passing through the nanopore. The depth and the frequency of the pulse signal are proportional to the particle volume and the particle concentration, respectively (Fig. 1). The depth of the pulse signal varies by approximately 0.5 nA, suggesting the presence of slightly different sized particles.

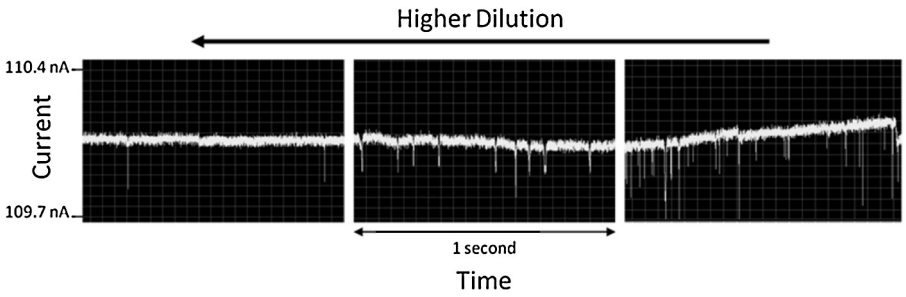

Fig. 1. Pulse events of carboxylated polystyrene microspheres at different dilutions. The dips in current signal represent particle translocation events. The particle concentration decreases in the direction of the arrow located at the top of the signal plots. The baseline current is around 110 nA. The abscissas of three plots are in the scale of 1 s. These plots are a subset of recorded signal data. Some pulse signals, as in the right plot, appear to drop under the lower limit of the plot, but the recorded signal data captures complete pulse signal.

Based on the current readouts, the flow rates of microspheres were measured and compared with the particle numbers derived from the concentration of original sample and dilution factor. The observed linear relationship between measured flow rates and estimated particle concentration (Fig. 2) reflected the accuracy of TRPS measurements to quantify particle concentration. The linear detection range of TRPS spanned from 10^7 to 10^{10} particles/ml.

The current readouts were also used to measure the size distributions of microsphere samples. To assess the accuracy of size measurements by TRPS, two different sized carboxylated polystyrene microspheres with a diameter of 70 nm (S) and 110 nm (B) were mixed at different ratios and analyzed. The size distributions were obtained from 185 to 680 particles using 100 nm calibration microspheres. The mean of the measured size distribution of homogenous samples agreed with the expected particle sizes (Fig. 3a). When these different sized beads were mixed in S-to-B concentration ratio of 5-to-1, 1-to-1 and 1-to-10, a bimodal population distribution was observed (Fig. 3b). One mode appeared at 70 nm and the other at 110 nm, as expected. The relative numbers of S and B particles correlated fairly well with expected mixture ratios, showing the accuracy of TRPS size measurements.

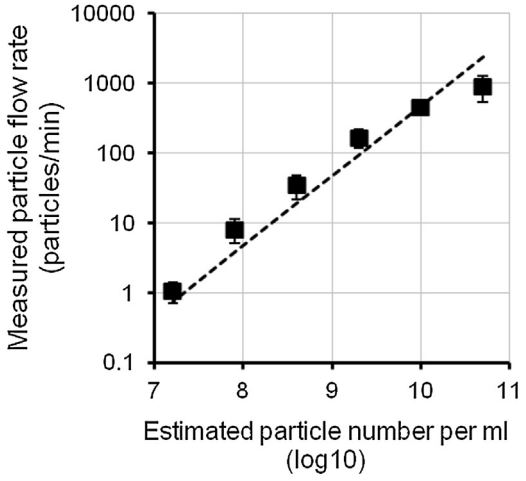

Fig. 2. Particle flow rate of carboxylated polystyrene microspheres measured by TRPS. Measured particle flow rates of microspheres (ordinate) were compared with the particle concentration (abscissa) that was estimated based on the concentration of original sample and dilution factor (squares, $n = 3$). The dashed line ($y = 4.68 \times 10^{-8}x$, $R^2 = 0.939$) indicated the linear relationship between the estimated particle concentration and the measured particle flow rate.

3.2. Comparison of TRPS and TEM for the quantitation of microsphere and virus populations

As a second part of the assessment of TRPS measurements, the particle concentrations of microsphere and virus populations measured by TRPS were compared with that determined by TEM. First, the concentration of the dilutions of a microsphere sample was analyzed. Both techniques measured the linear increase in particle number per ml with the increasing concentration of carboxylated polystyrene microspheres (Fig. 4). However, particle counts by TRPS spanned from 10^7 to 10^{10} particles/ml, a ~50-fold broader range than TEM measurements. Furthermore, coefficient of variation of TRPS measurements was found to be lower than that of TEM (Table 1) indicating that particle counts by TRPS were less variable than TEM.

The analysis was then extended to virus samples, where both TRPS and TEM were used to quantify the dilutions of a VSV sample. In both methods, 100 nm carboxylated polystyrene microsphere samples were used as calibration standards. As shown in Fig. 5, the results of TEM and TRPS agreed well and exhibited the expected linear trend between relative concentration and measured particle concentrations. However, TEM counts were again more variable than TRPS, particularly for the most dilute samples (Table 1).

Finally, the size distribution of virus population was examined by TRPS and TEM. The diameter and length of VSV particles were determined from the TEM images of VSV (Fig. 6a). Calculating the volume of a VSV particle by approximating its shape to a bullet (a half sphere on top of a cylinder) allowed the estimation of the equivalent particle diameter (EPD) that reflects the diameter of a sphere with an equivalent volume. The mean EPD of VSV was measured as 111.8 nm by TEM (Fig. 6b, $n = 14$), in agreement with the previous studies (Daaboul et al., 2014; Ge et al., 2010). This value also agreed well with TRPS measurements, which had a mean of 107.8 nm (Fig. 6c, $n = 1540$). Interestingly, the EPD distribution of VSV as quantified by TRPS spanned from 70 to 200 nm that match the diameter and length of VSV particles measured by TEM as 68

Table 1
Coefficient of variation of TEM and TRPS measurement of microsphere and VSV counts.

Relative concentration	Microsphere counts		VSV counts	
	TEM	TRPS	TEM	TRPS
1	0.43	0.05	0.42	0.42
0.2	0.19	0.33	0.79	0.09
0.04	0.87	0.02	0.96	0.29
0.008	0.98	0.27	0.54	0.37
0.0016	–	0.64	–	0.38
0.00032	–	–	–	0.34

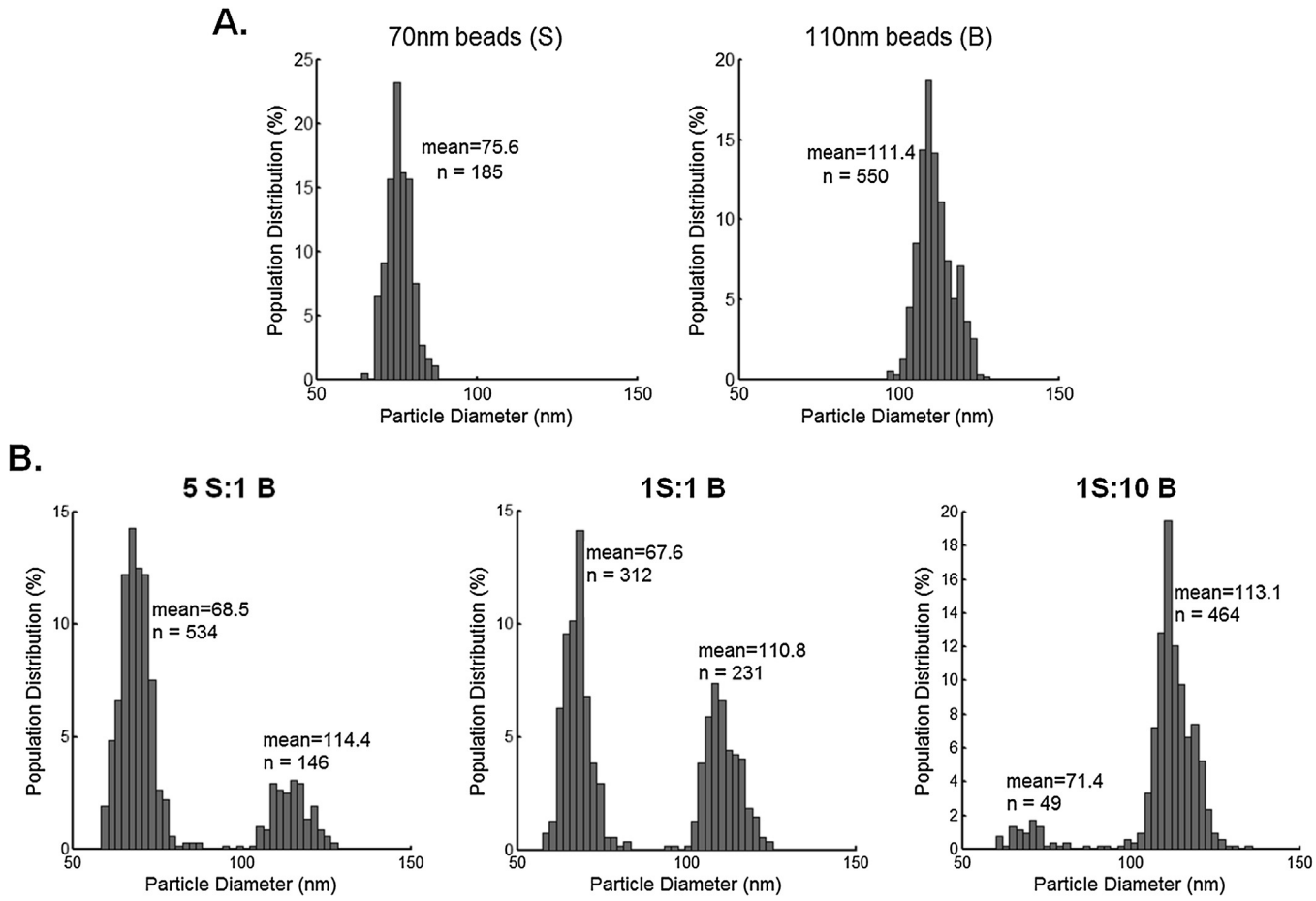

Fig. 3. The size distributions of carboxylated polystyrene microsphere mixtures measured by TRPS. The abscissas represent the particle diameter. Ordinates indicate the frequency of particle translocation events. The mean of measured particle diameters of different size bead population and the sample size (n) are given next to the distributions. (A) Distributions of homogenous samples of 70 nm (S, $n = 185$) and 110 nm (B, $n = 550$) beads. (B) Distributions of the bead mixtures. The ratios of the concentration of S to B in mixtures from left to right are 5-to-1, 1-to-1 and 1-to-10.

and 168 nm, respectively. The overlap between the range of EPD determined by TEM and TRPS suggested the reliability of TRPS to analyze the size distribution of virus populations.

3.3. Determination of total-to-infectious particle ratio in VSV populations

Following the validation of the accuracy of particle quantitation by TRPS, the virus particle counts by TRPS were compared with infectious unit concentrations measured by plaque assay and the total-to-infectious particle ratio in VSV populations was determined. Based on the analysis of six replicate populations, the total-to-infectious particle ratio was found to be 2.9 (Table 2). To explore the potential reasons for high total-to-infectious particle ratio, the presence of defective interfering particles (DIPs) in virus population (Timm et al., 2013) and the limitations of plaque assay were investigated. TEM or interference assay did not detect any DIP in virus samples eliminating the possibility of the contribution of DIPs to total-to-infectious particle ratio in the analyzed virus samples. On the other hand, the analysis on the current setup of plaque assay using VSV and BHK-21 cell lines indicated that only ~40% added virus can adsorb on cell monolayers over the typical range of virus dilutions used in plaque assay (data not shown), consistent with the findings of a previous study (Allison

Table 2
Virus titers of VSV populations measured by TRPS and plaque assay.

VSV population replicates	Virus titer per ml		Total-to-infectious particle ratio
	Particle counts by TRPS	Infectious units by plaque assay	
1	9.4×10^9	9.5×10^9	0.99
2	2.9×10^{10}	8.3×10^9	3.53
3	2.3×10^{10}	5.0×10^9	4.64
4	1.5×10^{10}	6.0×10^9	2.58
5	1.5×10^{10}	1.2×10^{10}	1.29
6	2.5×10^{10}	5.8×10^9	4.42
Average	$1.9 \times 10^{10} \pm 6 \times 10^9$	$7.7 \times 10^9 \pm 2.4 \times 10^9$	2.91 ± 1.42

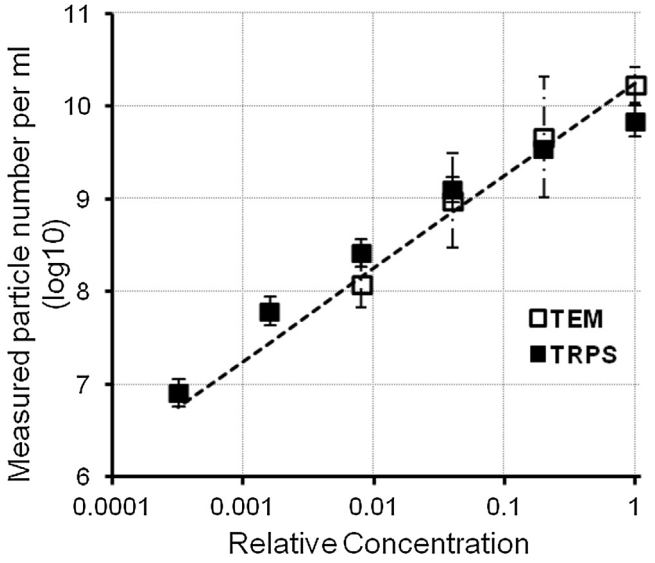

Fig. 4. TEM and TRPS counts of microsphere samples. Particle concentrations measured by TEM (open squares ($n = 2$), dashed error bars) and TRPS (filled squares ($n = 3$), solid error bars) for dilutions of a microsphere sample (abscissa) are shown. The dashed line is a linear curve fitted to the data. Dashed line: $y = 1.73 \times 10^{10}x$ (TRPS: $R^2 = 0.976$, TEM: $R^2 = 0.991$).

and Valentine, 1960). Such saturation effect would result in ~2.5-fold difference between the measurements by plaque assay and the actual virus concentration in tested sample, which is close to what was measured in this study, suggesting that all VSV particles are infectious.

4. Discussion

In the study of virus populations, TRPS provides clear advantages over TEM, allowing the high-throughput and accurate quantitation of particles across a 50-fold broader concentration range as examined in this work.

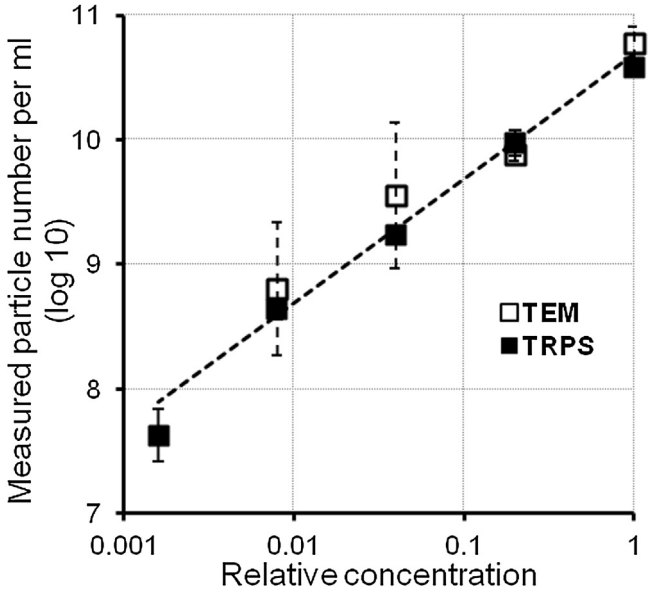

Fig. 5. VSV particle numbers measured by TRPS and TEM. A linear curve (dashed line, $y = (4.85 \times 10^{10})x$, TRPS: $R^2 = 0.927$, TEM: $R^2 = 0.816$) was fitted to the VSV particle concentrations measured by TEM (open squares ($n = 2$)) or TRPS (filled squares ($n = 3$)). Error bars of TEM and TRPS are shown as dashed and solid lines, respectively.

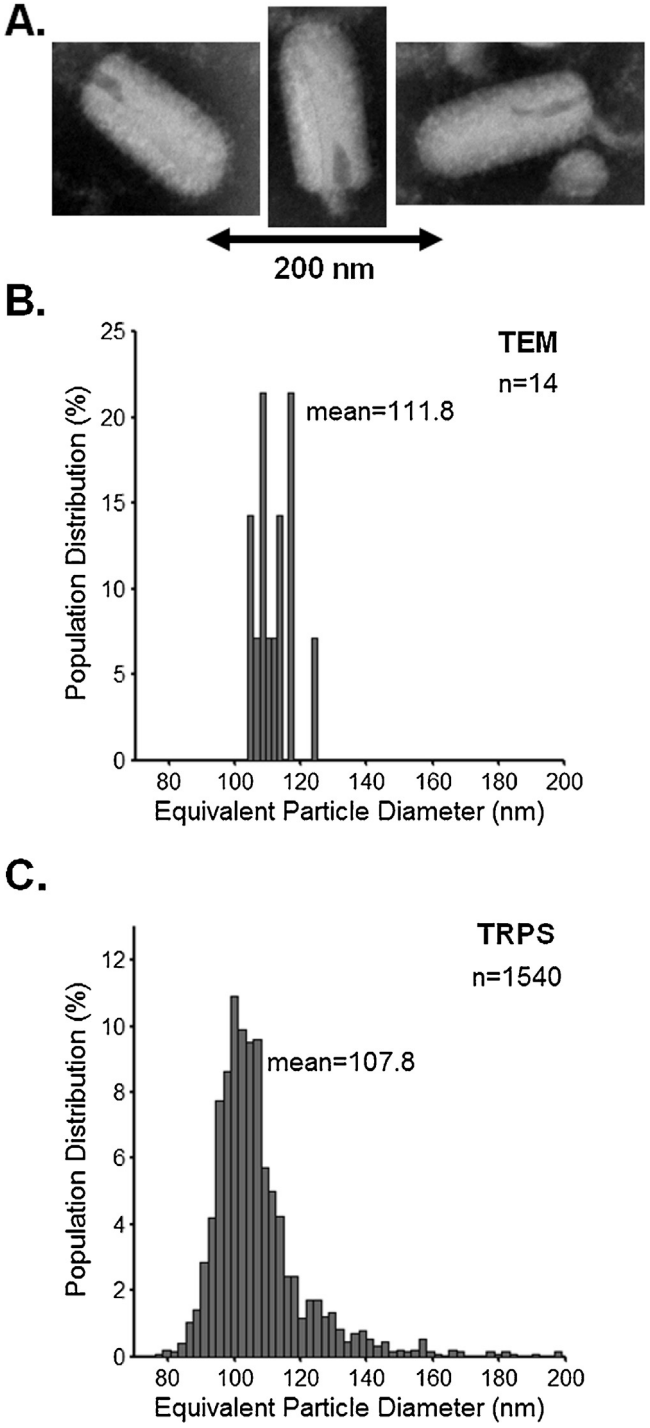

Fig. 6. Size measurement of VSV population by TEM and TRPS. (A) Three representative TEM images of VSV particles are shown. (B) The equivalent particle diameter (EPD, abscissa) distribution of VSV population was estimated by approximating the shape of the VSV particles to a bullet (a half sphere on top of a cylinder) using measured diameter and length of 14 VSV particles by TEM ($n = 14$). The mean equivalent particle diameter was calculated as 111.8 nm, as indicated on the plot. (C) The EPD distribution was measured by TRPS ($n = 1540$) and the mean EPD was calculated as 107.8 nm.

When compared with TEM, TRPS provided a larger sample size that enabled more accurate quantitation of virus particles. For virus samples at moderate concentrations TRPS collected information from hundreds of particles, as opposed to tens of particles by TEM. Additionally, TEM micrographs of relatively dilute sample (5×10^8 particles/ml) contained one particle in 30 TEM

micrographs leading to high variability as observed especially in the lowest two counts by TEM in Fig. 5. On the contrary, TRPS counted 40 particles during a 2-min long run of the same sample. The effective sample size of TRPS can further be improved by allowing the sample to run for a longer time. Such high-throughput characteristic of TRPS is crucial for accurate measurements.

High-throughput feature of TRPS was also observed in its ability to collect and process information in a shorter time as compared to TEM. The data acquisition and processing of each sample by TRPS and TEM took 15 and 60 min, respectively. Notwithstanding the additional 15–30 min for the start-up of the TRPS to maintain a uniform particle flow rate, TRPS still provided clear advantage over TEM in terms of time and effort, particularly for multiple sample analysis.

TRPS enabled the quantitation of virus samples as dilute as 10^7 particles/ml, which was 50-fold lower than the lower detection limit of TEM. The improvement in particle detection range benefits the quantitation of the virus infection yield, which can vary depending on the virus strain and infection conditions (Timm and Yin, 2012; Wagner et al., 1963). However, the upper detection limit by TRPS was found to be lower than that of TEM. During the runs of the high concentration samples (Fig. 2 upper limit), the particle flow rate became less uniform, possibly due to the temporary clogging of the nanopore. Diluting these concentrated samples helped to avoid the irregularity in particle flow and to accurately quantify particle concentration.

The measurements of total virus particle and infectious unit concentrations by TRPS and plaque assay indicated a 2.9-fold difference between total and infectious VSV particle numbers. In other virus-cell systems, even higher total-to-infectious particle ratios have been observed (Heider and Metzner, 2014). The realistic interpretation of this ratio requires a good understanding of the limitations of the measurement methods and segregation of these limitations from the biological implications. However, little attention has been paid to the possible contribution of the limitations of traditional infectivity assays (such as TCID50 and plaque assay) to total-to-infectious particle ratio. In this study, this ratio was evaluated considering the accuracy of both TRPS and plaque assay and indicated that VSV is a highly efficient virus in terms of infectivity.

In conclusion, TRPS successfully measured particle concentration and size distribution of virus populations in a particle concentration range spanning from 10^7 to 10^{10} particles/ml (and higher when diluted) and provided less variable and higher throughput analysis of virus populations as compared to TEM. This study highlights the potential of TRPS technology to study virus populations on the basis of physical particles, which is a common measure to characterize the diverse virus populations that emerge during various virus infections.

Acknowledgements

The authors are grateful to Randall Massey at Medical School Electron Microscopy Facility for his technical assistance in TEM imaging. This work was supported by grants from the U.S. National Institutes of Health (AI091646 and AI104317).

References

Allison, A., Valentine, R., 1960. Virus particle adsorption: III. Adsorption of viruses by cell monolayers and effects of some variables on adsorption. Biochim. Biophys. Acta 40, 400–410, http://dx.doi.org/10.1016/0006-3002(60)91380-9.

Anderson, W., Kozak, D., Coleman, V.A., Jämting, Å.K., Trau, M., 2013. A comparative study of submicron particle sizing platforms: accuracy, precision and resolution analysis of polydisperse particle size distributions. J. Colloid Interface Sci. 405, 322–330, http://dx.doi.org/10.1016/j.jcis.2013.02.030.

Arjmandi, N., Van Roy, W., Lagae, L., 2014. Measuring mass of nanoparticles and viruses in liquids with nanometer-scale pores. Anal. Chem. 86, 4637–4641, http://dx.doi.org/10.1021/ac500396t.

Bell, N.C., Minelli, C., Tompkins, J., Stevens, M.M., Shard, A.G., 2012. Emerging techniques for submicrometer particle sizing applied to stober silica. Langmuir 28, 10860–10872.

Carpenter, J.E., Henderson, E.P., Grose, C., 2009. Enumeration of an extremely high particle-to-PFU ratio for Varicella-zoster virus. J. Virol. 83, 6917–6921, http://dx.doi.org/10.1128/JVI.00081-09.

Daaboul, G.G., Lopez, C.A., Chinnala, J., Goldberg, B.B., Connor, J.H., Unlü, M.S., 2014. Digital sensing and sizing of vesicular stomatitis virus pseudotypes in complex media: a model for ebola and marburg detection. ACS Nano 8, 6047–6055, http://dx.doi.org/10.1021/nn501312q.

DeBlois, R.W., 1970. Counting and sizing of submicron particles by the resistive pulse technique. Rev. Sci. Instrum. 41, 909, http://dx.doi.org/10.1063/1.1684724.

Galasso, G.J., Sharp, D.G., 1962. Virus particle aggregation and the plaque-forming unit. J. Immunol. 88, 339–347.

Gazzola, D., Van Sluyter, S.C., Curioni, A., Waters, E.J., Marangon, M., 2012. Roles of proteins, polysaccharides, and phenolics in haze formation in white wine via reconstitution experiments. J. Agric. Food Chem. 60, 10666–10673, http://dx.doi.org/10.1021/jf302916n.

Ge, P., Tsao, J., Schein, S., Green, T.J., Luo, M., Zhou, Z.H., 2010. Cryo-EM model of the bullet-shaped vesicular stomatitis virus. Science 327, 689–693, http://dx.doi.org/10.1126/science.1181766.

Heider, S., Metzner, C., 2014. Quantitative real-time single particle analysis of virions. Virology 462/463, 199–206, http://dx.doi.org/10.1016/j.virol.2014.06.005.

Henriquez, R.R., Ito, T., Sun, L., Crooks, R.M., 2004. The resurgence of Coulter counting for analyzing nanoscale objects. Analyst 129, 478–482, http://dx.doi.org/10.1039/B404251B.

Kozak, D., Anderson, W., Vogel, R., Trau, M., 2011. Advances in resistive pulse sensors: devices bridging the void between molecular and microscopic detection. Nano Today 6, 531–545, http://dx.doi.org/10.1016/j.nantod.2011.08.012.

Smith, K.O., Melnick, J.L., 1962. Electron microscopic counting of virus particles by sedimentation on aluminized grids. J. Immunol. 89, 279–284.

Sowerby, S.J., Broom, M.F., Petersen, G.B., 2007. Dynamically resizable nanometre-scale apertures for molecular sensing. Sens. Actuators B: Chem. 123, 325–330.

Terejanszky, P., Makra, I., Furjes, P., Robert, G., 2014. Calibration-less sizing and quantitation of polymeric nanoparticles and viruses with quartz nanopipets. Anal. Chem. 86, 4688–4697.

Timm, A., Yin, J., 2012. Kinetics of virus production from single cells. Virology 424, 11–17, http://dx.doi.org/10.1016/j.virol.2011.12.005.

Timm, C., Akpinar, F., Yin, J., 2013. Quantitative characterization of defective virus emergence by deep sequencing. J. Virol., http://dx.doi.org/10.1128/JVI.02675-13.

Van Bracht, E., Raavé, R., Verdurmen, W.P.R., Wismans, R.G., Geutjes, P.J., Brock, R.E., Oosterwijk, E., van Kuppevelt, T.H., Daamen, W.F., 2012. Lyophilisomes as a new generation of drug delivery capsules. Int. J. Pharm. 439, 127–135, http://dx.doi.org/10.1016/j.ijpharm.2012.10.008.

Vogel, R., Willmott, G., Kozak, D., Roberts, G.S., Anderson, W., Groenewegen, L., Glossop, B., Barnett, A., Turner, A., Trau, M., 2011. Quantitative sizing of nano/microparticles with a tunable elastomeric pore sensor. Anal. Chem. 83, 3499–3506, http://dx.doi.org/10.1021/ac200195n.

Wagner, R.R., Levy, A.H., Snyder, R.M., Ratcliff, G.A., Hyatt, D.F., 1963. Biologic properties of two plaque variants of vesicular stomatitis virus (Indiana serotype). J. Immunol. 91, 112–122.

Watson, D.H., Russell, W.C., Wildy, P., 1963. Electron microscopic particle counts on herpes virus using the phosphotungstate negative staining technique. Virology 19, 250–260.

Wertz, G.W., 1998. Gene rearrangement attenuates expression and lethality of a nonsegmented negative strand RNA virus. Proc. Natl. Acad. Sci. U. S. A. 95, 3501–3506, http://dx.doi.org/10.1073/pnas.95.7.3501.